

LETTER TO THE EDITOR

Detection of pancreatic cancer by indocyanine green-assisted fluorescence imaging in the first and second near-infrared windows

Dear Editor,

In the United States, pancreatic cancer is considered the fourth most common reason for cancer-related deaths; over 53% of patients are diagnosed at end-stage with a 5-year survival rate of less than 3% [1]. Incomplete removal of all cancerous cells generally leads to local recurrence of pancreatic cancer [2]. Thus, the detection of tumor margin status plays an essential role in the complete resection of pancreatic cancer. Most of the existing imaging modalities, like computed tomography and magnetic resonance imaging, are primarily used for preoperative planning; these modalities also have issues of bulky equipment, radiation concerns, and slow imaging speed [2]. Thus, these modalities can neither provide an intraoperative diagnosis of cancer with high sensitivity and specificity nor be used to define tumor margins [3].

Indocyanine green (ICG), a clinically approved fluorescent dye, has become a popular choice in various clinical applications, e.g., dental imaging [4, 5]. Many studies suggested that ICG could become an ideal fluorescent agent to enhance the imaging contrast between normal tissues and certain tumors, such as breast cancer, gastric cancer, head and neck cancer, and pancreatic tumor [6]. However, most of the existing studies using ICG performed the imaging in the first near-infrared window (NIR-I, 700–1000 nm) [6]. Compared to traditional NIR-I, imaging in the second NIR window (NIR-II, 1000–1700 nm) could achieve a deeper tissue penetration depth and acquire good imaging quality because of its low autofluorescence and photon scattering [7], especially with ICG [8]. Existing studies reported ICG-assisted NIR fluorescence imaging in NIR-II (ICG-NIRF-II) for the detection of thoracic malignancy [9] and

human dental diseases [4]. To our best knowledge, no previous study has reported the use of ICG-NIRF-II to image pancreatic cancer in humans. In this letter, we designed an ICG-NIRF imaging system (**Figure 1A**) and used the U.S. Food and Drug Administration (FDA)-approved ICG as the fluorescent agent to image murine and human pancreatic cancers in both NIR-I and NIR-II (**Supplementary file**).

Nine patients diagnosed with pancreatic neuroendocrine tumor (PNET) and 1 with pancreatic ductal adenocarcinoma (PDAC) (stage I–III) at the Ochsner Medical Center-Kenner of Louisiana State University Health Sciences Center (New Orleans, LA, USA) were enrolled. Human tumor specimens were collected during standard-of-care surgical procedures. Under light microscope, the excised PNET was more solid with a deeper staining in purple blue color, due to the hyperplasia of tumor cells, than the adjacent normal pancreatic tissue (**Supplementary Figure S1**).

Informed written consent was obtained from each patient. For patients with PNET, 7 were dosed with ICG at 0.22 mg/kg and 2 at 0.50 mg/kg through intravenous injection. The patient with PDAC was dosed with ICG at 0.22 mg/kg. Intraoperative *ex vivo* imaging of tumor and tumor margins was then performed. Ten female immunocompetent athymic nude Nu/J mice of about 6–8 weeks old, transplanted with CFPAC-1 cells, were used as the animal model for ICG-NIRF imaging with 0.22 mg/kg.

In the mouse model, tumor tissues demonstrated higher fluorescence intensity than normal tissues under both ICG-NIRF-I and ICG-NIRF-II imaging. In the short imaging window (4 h), ICG-NIRF-II had a higher tumor-background ratio (TBR) of the fluorescence peak intensities than ICG-NIRF-I (4.30 ± 0.38 vs. 2.16 ± 0.06); ICG-NIRF-I had a higher TBR in the long imaging window (24 h) than in the short imaging window (11.42 ± 1.28 vs. 2.16 ± 0.06) (**Figure 1B–D**). Thus, all those TBRs (>2.0) of the short and long imaging windows indicate that tumors were positive under both ICG-NIRF-I and ICG-NIRF-II imag-

List of abbreviations: NIR, near-infrared; ICG, Indocyanine green; NIR-I, short near-infrared window I (700–1000 nm); NIR-II, long near-infrared window II (1000–1700nm); ICG-NIRF-I, ICG near-infrared-fluorescent imaging at NIR-I; ICG-NIRF-II, ICG near-infrared-fluorescent imaging at NIR-II; InGaAs, Indium gallium arsenide

This is an open access article under the terms of the [Creative Commons Attribution-NonCommercial-NoDerivs](https://creativecommons.org/licenses/by-nc-nd/4.0/) License, which permits use and distribution in any medium, provided the original work is properly cited, the use is non-commercial and no modifications or adaptations are made.

© 2021 The Authors. *Cancer Communications* published by John Wiley & Sons Australia, Ltd. on behalf of Sun Yat-sen University Cancer Center

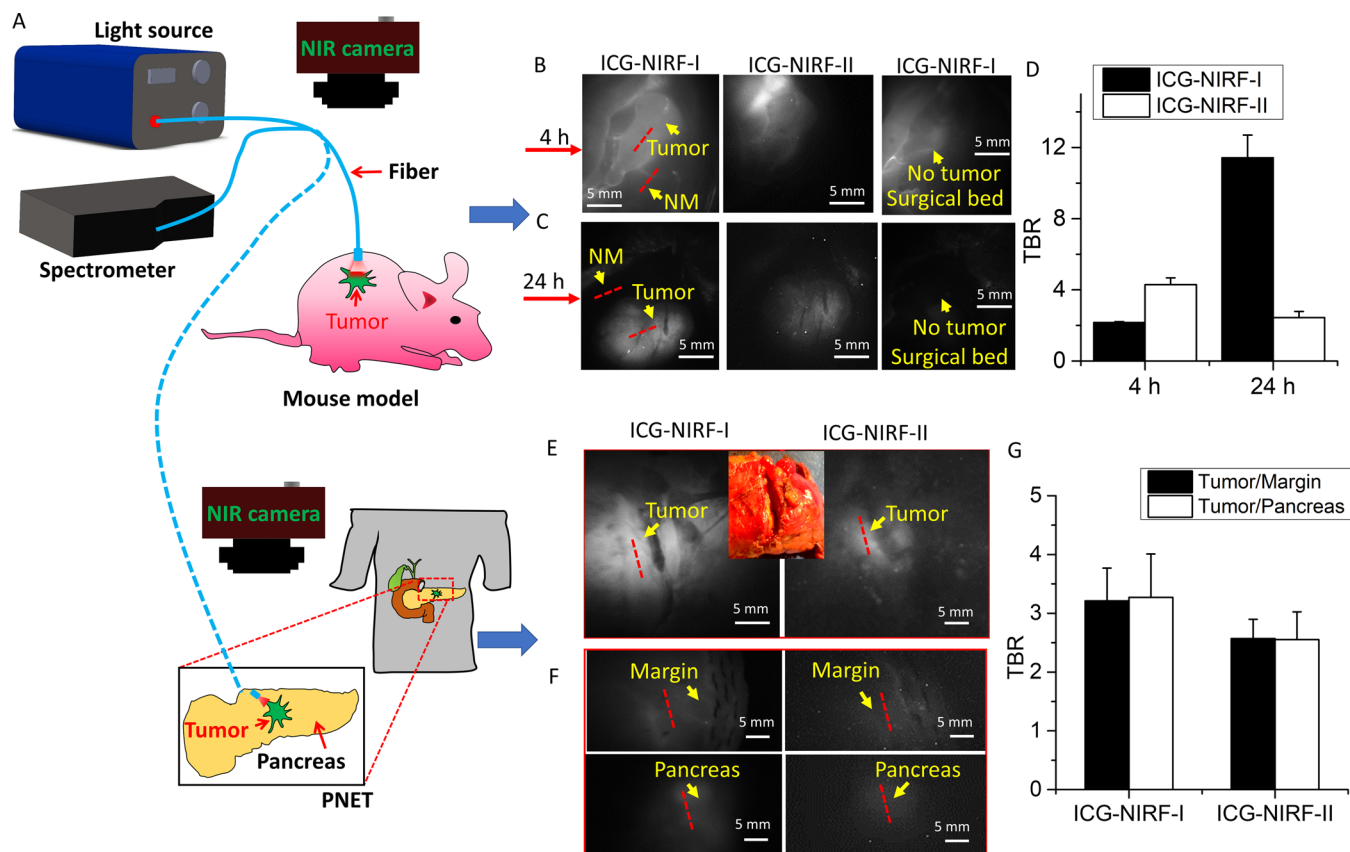


FIGURE 1 Detection of murine and human PNET with ICG-NIRF imaging. (A) Schematic diagram of the ICG-NIRF imaging system. (B-C) Images of murine model at 4 h (B) and 24 h (C) after ICG injection in NIR-I and -II windows. (D) TBR of tumor to normal tissues of murine model in ICG-NIRF-I and -II imaging. (E-F) Images of human (Subject 6) PNET tissues (E) and tumor margin and normal pancreatic tissues (F) in NIR-I and -II windows. (G) TBR of PNET to tumor margin and normal pancreas in human patients (Subject 6) at the imaging window of 7 h. Imaging conditions: laser power 170 mW, 40 ms exposure time for ICG-NIRF-I imaging and 30 ms exposure time for ICG-NIRF-II imaging. Abbreviations: ICG-NIRF: indocyanine-green near-infrared fluorescence, NIR-I/-II: near-infrared-first/-second windows, NM: normal tissues near tumors; PNET: pancreatic neuroendocrine tumors; TBR: tumor-background fluorescence ratio.

ing, which was consistent with the definition in previously published studies on other cancer types[10].

In human patients, we found that both ICG-NIRF-I and ICG-NIRF-II imaging could identify PNET: the tumor tissues showed brighter fluorescence than normal tissues (including tumor margin and normal pancreatic tissues); the margins had similar fluorescence intensity to the normal pancreatic tissues, indicating negative margins, which were confirmed by histopathology (Figure 1F-G). The human PDAC also showed similar trend in ICG-NIRF-I and ICG-NIRF-II imaging (Supplementary Figure S2). Similar to the mouse model, both types of human pancreatic tumors had positive TBR values (>2.0) of the tumor to normal tissues (Figure 1G and Supplementary Figure S2E).

Compared with other fluorescent dyes (e.g., 5-aminolevulinic acid), ICG has already been approved by the US FDA, which could result in faster clinical translation than a completely new synthetic dye [8]. We

successfully demonstrated that ICG-NIRF imaging could image pancreatic tumors in both NIR-I and -II. Particularly, our results indicated that in the short imaging window, ICG-NIRF-II had better image quality (larger TBR) than ICG-NIRF-I. This is due to the lower autofluorescence and light scattering in NIRF-II than in NIRF-I [9]. In the long imaging window, the advantage of NIRF-II vanished since this scheme employs the off-peak emission of ICG and we employed a low ICG dose (0.22 mg/kg); after long intervals of ICG injection, the ICG molecules in the tissues were in such low concentrations that the fluorescence was comparable to the InGaAs camera sensor noise level [9]. The long imaging window can acquire better image quality in ICG-NIRF-I imaging than in ICG-NIRF-II imaging, and only the tumor remained bright at that time.

According to existing studies, the most common explanation for ICG accumulating in tumors at 24 h after injection is their enhanced permeability and retention effect

[6]. When ICG is injected into the blood vessel, it would not have any known metabolites and just bind with lipid or lipoprotein complexes, and the bound protein acts as a macromolecule [6]. Because of defective leaky capillaries in the tumor, these macromolecules become trapped in the tumors while most ICG molecules are cleared from the normal tissues [6]. Thus, in the long imaging window, high ICG concentration in tumors and almost no ICG in normal tissues can cause great difference in fluorescence signals between cancerous and non-cancerous tissues, contributing to better image quality in ICG-NIRF-I imaging in the long imaging window than in the short imaging window.

Compared to the short imaging window, ICG molecules would gradually be extracted by the liver into bile juice [6], and the extracted ICG molecules could lead to decreased ICG concentration (also decrease the fluorescence signals) in the tumor in the long imaging window. Therefore, the TBR of ICG-NIRF-II becomes smaller in the long imaging window than in the short imaging window.

Although ICG is generally considered safe, the US FDA recommends that the ICG dose be ≤ 2 mg/kg; adverse effects of ICG were mainly reported when the ICG dose exceeded 1 mg/kg [9]. The ICG dose used in the present study was much lower than doses used in previous studies (usually 2-5 mg/kg) [9]. Evaluating ICG-NIRF imaging performance at such low ICG doses is meaningful to clinical translation. The image quality of ICG-NIRF-II imaging could be improved if the ICG dose increased, especially in human patients, which was confirmed in the present study when the ICG dose was increased from 0.22 to 0.50 mg/kg (Supplementary Figure S3).

Overall, the present study demonstrated the feasibility of using ICG as a fluorescent agent at low doses (≤ 0.5 mg/kg) to distinguish pancreatic tumors from normal tissues in both NIR-I and NIR-II for mouse models and human patients. ICG-NIRF imaging has the potential to become a novel image-guiding tool for the diagnosis of pancreatic cancer.

DECLARATIONS

Ethics approval and consent to participate.

Not applicable.

CONSENT FOR PUBLICATION

Not applicable.

COMPETING INTERESTS

The authors declare that they have no competing interests.

ACKNOWLEDGMENTS

We thank Sherry Ring from LSU Department of Comparative Biomedical Science for her contribution to the preparation of pathohistology slides of the mice. This research was supported by Louisiana State University Economic Development Assistantships (000398), LSU Leveraging Innovation for Technology Transfer (LIFT2) Grant (LSU-2021-LIFT-009, LSU-2020-LIFT-008), Health Sciences Center New Orleans, Louisiana State University Grant (HSCNO-2019-LIFT-004), Louisiana Board of Regents Grant (LEQSF (2018-21)-RD-A-09, LEQSF(2020-21)-RD-D-02), NIH (1U01AA029348-01), NSF CAREER award (2046929).

AUTHOR CONTRIBUTIONS

Z. Li contributed to experimental design, data acquisition, analysis, and interpretation, drafted the manuscript. Z. Li contributed to data acquisition, analysis and interpretation, drafted the manuscript. A. Ramos contributed to data analysis, interpretation and drafted the manuscript. J. P. Boudreaux contributed to data acquisition and proofread the manuscript. R. Thiagarajan contributed to data acquisition and proofread the manuscript. Y. Bren-Mattison contributed to data acquisition and proofread the manuscript. M. E. Dunham contributed to data interpretation and proofread the manuscript. A. J. McWhorter contributed to data interpretation and proofread the manuscript. Q. Chen contributed to CNN model improvement, data acquisition and interpretation, drafted the manuscript. J. Zhang contributed to CNN model improvement, data interpretation, and proofread the manuscript. X. Li contributed to data interpretation and revision of the manuscript, J. Feng contributed to data interpretation and revision of the manuscript. Y. Li contributed to data analysis and revision of the manuscript. S. Yao contributed to data interpretation and revision of the manuscript. J. Xu contributed to conception, experimental design, data interpretation, critical revision of the manuscript.

Zhongqiang Li¹

Zheng Li¹

Alexandra Ramos²

J. Philip Boudreaux³


Ramcharan Thiagarajan³

Yvette Bren Mattison³

Michael E. Dunham⁴

Andrew J McWhorter⁴

Qing Chen⁵

Jian Zhang⁵ 

Ji-Ming Feng²

Yanping Li⁶

Shaomian Yao²

Jian Xu¹ 

- ¹ Division of Electrical and Computer Engineering, College of Engineering, Louisiana State University, Baton Rouge, LA 70803, USA
- ² Department of Comparative Biomedical Science, School of Veterinary Medicine, Louisiana State University, Baton Rouge, LA 70803, USA
- ³ Department of Surgery, School of Medicine, Louisiana State University Health Science Center, New Orleans, LA 70112, USA
- ⁴ Department of Otolaryngology, School of Medicine, Louisiana State University Health Science Center, New Orleans, LA 70112, USA
- ⁵ Division of Computer Science & Engineering, College of Engineering, Louisiana State University, Baton Rouge, LA 70803, USA
- ⁶ School of Environment and Sustainability, University of Saskatchewan, Saskatoon, SK S7N 5C9, Canada

Correspondence

Jian Xu, Division of Electrical and Computer Engineering, College of Engineering, Louisiana State University, Baton Rouge, LA 70803, USA.
Email: jianxu1@lsu.edu

ORCID

Jian Zhang  <https://orcid.org/0000-0002-6595-8602>

Jian Xu  <https://orcid.org/0000-0001-6962-5146>

REFERENCES

1. Society, AC, Cancer Facts & Figures 2020. 2020: The Society.
2. Xu, J, DA Kooby and S Nie. Nanofluorophore Assisted Fluorescence Image-guided Cancer Surgery. *J Med-Clin Res & Rev.* 2018; 2(1): 1-3.

3. Pandya, AK, GK Serhatkulu, A Cao, RE Kast, H Dai, R Rabah, et al. Evaluation of pancreatic cancer with Raman spectroscopy in a mouse model. *Pancreas.* 2008; 36(2): e1-8.
4. Li, Z, S Yao and J Xu. Indocyanine-green-assisted near-infrared dental imaging - the feasibility of in vivo imaging and the optimization of imaging conditions. *Sci Rep.* 2019; 9(1): 8238.
5. Li, Z, W Zaid, T Hartzler, A Ramos, ML Osborn, Y Li, et al. Indocyanine green-assisted dental imaging in the first and second near-infrared windows as compared with X-ray imaging. *Ann N Y Acad Sci.* 2019; 1448(1): 42-51.
6. Alander, JT, I Kaartinen, A Laakso, T Patila, T Spillmann, VV Tuchin, et al. A review of indocyanine green fluorescent imaging in surgery. *Int J Biomed Imaging.* 2012; 2012: 940585.
7. Cao, J, B Zhu, K Zheng, S He, L Meng, J Song, et al. Recent Progress in NIR-II Contrast Agent for Biological Imaging. *Front Bioeng Biotechnol.* 2019; 7: 487.
8. Starosolski, Z, R Bhavane, KB Ghaghada, SA Vasudevan, A Kaay and A Annapragada. Indocyanine green fluorescence in second near-infrared (NIR-II) window. *PLoS One.* 2017; 12(11): e0187563.
9. Newton, AD, JD Predina, CJ Corbett, LG Frenzel-Sulyok, L Xia, EJ Petersson, et al. Optimization of Second Window Indocyanine Green for Intraoperative Near-Infrared Imaging of Thoracic Malignancy. *J Am Coll Surg.* 2019; 228(2): 188-197.
10. Newton, AD, JD Predina, MH Shin, LG Frenzel-Sulyok, CM Vollmer, JA Drebin, et al. Intraoperative Near-infrared Imaging Can Identify Neoplasms and Aid in Real-time Margin Assessment During Pancreatic Resection. *Ann Surg.* 2019; 270(1): 12-20.

SUPPORTING INFORMATION

Additional supporting information may be found in the online version of the article at the publisher's website.